Gas-Phase Kinetic Studies of Tetralin Hydrogenation on Pt/Alumina

ARTICLE *in* INDUSTRIAL & ENGINEERING CHEMISTRY RESEARCH · SEPTEMBER 2005

Impact Factor: 2.59 · DOI: 10.1021/ie0500873

4 AUTHORS, INCLUDING:

Siriporn Jongpatiwut
Chulalongkorn University
25 PUBLICATIONS **304** CITATIONS
SEE PROFILE

Daniel E Resasco
University of Oklahoma
331 PUBLICATIONS **11,059** CITATIONS
SEE PROFILE

KINETICS, CATALYSIS, AND REACTION ENGINEERING

Gas-Phase Kinetic Studies of Tetralin Hydrogenation on Pt/Alumina

Roberto C. Santana,[†] Siriporn Jongpatiwut,[†] Walter E. Alvarez,[‡] and Daniel E. Resasco*[,†]

School of Chemical, Biological, and Materials Engineering, The University of Oklahoma, Norman, Oklahoma 73019, and ConocoPhillips Technology Center, Bartlesville, Oklahoma 74004

The hydrogenation of aromatic compounds is a reaction of relevance in the improvement of diesel fuel quality. In this work, the kinetics of tetralin (1,2,3,4-tetrahydronaphthalene) hydrogenation over Pt/Al_2O_3 catalysts have been studied in an integral fixed bed reactor at 500 psig in the temperature range 553−573 K. A semiempirical Langmuir−Hinshelwood equation has been used to model the kinetics. The values of the kinetic parameters were determined by a nonlinear fitting, while the heats of adsorption for the hydrocarbons involved (tetralin and *cis*- and *trans*-decalin) were experimentally obtained by temperature-programmed desorption. The adsorption competition between tetralin and the hydrogenated products (*cis*- and *trans*-decalin) for surface active sites can be quantitatively traced to the higher heat of adsorption of tetralin compared to those of *cis*- and *trans*-decalins. As a result, while the activation energy for the *cis*−*trans* isomerization is significantly lower than the one for tetralin hydrogenation and its intrinsic reaction rate much higher than that of hydrogenation, the isomerization reaction can only be observed when the concentration of tetralin in the gas phase is very much reduced. In consequence, at low conversions, the *trans*/*cis* ratio remains unchanged, and it only increases to its equilibrium value at very high tetralin conversions.

1. Introduction

Despite much interest and progress in the development of alternative energy resources, it is expected that conventional fuels such as diesel and gasoline will be the dominating fuels for many years. Diesel fuel has the advantage of higher energy efficiency, but its use has the associated problems of NO_x and particulate matter (PM) emissions, that are not straightforward to solve.[1] Aiming at 90% reduction in PM, NO_x, and hydrocarbon emissions in new vehicles, future regulations will require control of engines and fuels as combined systems.[2] For example, the amount of PM emissions from diesel engines can be reduced by decreasing the sulfur content of the fuel, raising the cetane number, and decreasing the aromatic content.[3] The last two factors are interconnected because reducing the content of aromatics significantly increases the cetane number.[4] Therefore, increased interest has recently developed on the saturation of aromatics present in middle distillates, such as light cycle oil (LCO). Hydrogenation of polynuclear aromatics to monoaromatics is easily achieved by conventional hydrotreating. Yet, the saturation of the final ring is by far more difficult due to the stabilization of the monoaromatic ring.[5−7] A recently proposed two-stage process contains a typical hydrotreating catalyst in the first stage (NiMo, NiW, CoMo) followed by a second stage of noble -metal catalyst, to ensure deep hydrogenation.[8] Unfortunately, noble-metal-based catalysts are rapidly poisoned by common contaminants found in industrial feeds such as organic sulfur and nitrogen compounds.[9−11] A fundamental understanding of the hydrogenation of the last ring will help accelerate the development of more effective deep hydrogenation catalysts. In previous work done by our group,[12] we found that *cis*-decalin is much more active and selective than *trans*-decalin toward ring opening. Therefore, to improve CN one might need to maximize the production of *cis*-decalin. It is important to monitor the resulting *cis*/*trans* decalin ratio in the hydrogenation step.

In this contribution, we have conducted a kinetic study using a semiempirical model, which may provide a better understanding of the hydrogenation of the last ring in polynuclear aromatics. We have used tetralin (TL) as a probe of the one-ring aromatic compounds present in diesel fuels.[6,7] One of the first mechanistic studies of the hydrogenation of TL was conducted by Weitkamp.[7] After that seminal work, some studies have been carried out on this reaction, and in most cases, the kinetics have been described by pseudo-first-order models[11,13−15] or power-law models.[16,17] A few authors[18] have used Langmuir−Hinshelwood (L−H) type models but have made no attempt to differentiate between the two possible paths to *cis*-decalin (CD) and *trans*-decalin (TD) nor to account for the role of the difference in adsorption of reactants and products. Recently, Rautanen et al.[19−22] have addressed, in a series of articles, the liquid-phase kinetic behavior of the hydrogenation of different aromatics on nickel catalysts. In those cases, the hydrogenation of TL was studied and fitted using

* To whom correspondence should be addressed. Phone: (405) 325-4370. E-mail: resasco@ou.edu.
[†] The University of Oklahoma.
[‡] ConocoPhilips Technology Center.

10.1021/ie0500873 CCC: $30.25
Published on Web 09/10/2005

three different models: power law, simplified L−H, and a mechanistic based model.[19] The hydrogenation of naphthalene[20] and mixtures of TL, naphthalene, and toluene[21] has been modeled using a simplified L−H-type expression. Alternatively, the kinetics of naphthalene and TL hydrogenation have been studied using a mechanistic-based model that features three possible types of adsorption modes of the aromatic on the active site.[22] In the liquid phase, internal mass transfer limitations can become a complication, and therefore in all these cases, the parameters obtained from the fitting may have been affected by intraparticle mass transfer resistances, and as a result, the uncertainty in the parameters thus derived may be high.

In the present study, conducted in the vapor phase, a semiempirical kinetic model has been used. While not as rigorous as the microkinetics studies performed in some systems,[23−26] it still provides physical significance to the parameters obtained from the fitting. For example, heats of adsorption have been obtained by a thermal desorption method while physical−chemical constraints have been imposed to the fittings to make the resulting parameters meaningful. Therefore, in contrast to previous studies, the parameters determined here have helped us get a better understanding of this reacting system.

2. Experimental Section

2.1. Catalyst Preparation. The catalyst employed in this study was a 0.4 wt % Pt/Al_2O_3, prepared by incipient wetness impregnation of an aqueous solution of hydrogen chloroplatinate hexahydrate (from Acros) over γ-alumina (from Saint-Gobian NorPro Corp; surface area = 252 m^2/g, pore diameter = 10.8 nm). Before impregnation, the γ-alumina support was ground and sieved to 20−35 mesh-size particles. For the impregnation procedure, the original Pt solution was diluted with deionized water to reach a liquid-to-support ratio of 1.3 mL/g. After impregnation and thorough mixing, the catalyst was first dried at room temperature for 4 h, then in an oven at 383 K for 12 h, and finally calcined in an oven at 573 K for 2 h. The BET analysis of the nitrogen adsorption measurements indicated that the surface area for the calcined Al_2O_3 is 198 m^2/g.

2.2. CO Chemisorption. Dynamic chemisorption of CO was used to estimate the metal dispersion on the catalyst. The CO uptake measurements were performed in a $^1/_4$ in. flow reactor made of quartz, containing 0.82 g of catalyst. Before exposure to CO, the samples were reduced in-situ under 100 SCCM of H_2 at 573 K for 1 h, and purged in flowing He, first at 573 K for 30 min and then cooled to room temperature. The stream was continuously monitored online by a mass spectrometer. Calibrated pulses of 250 μL of 5% CO in He were sent over the catalyst bed every 5 min, until the area of the (mass to charge) m/e = 28 peak stopped increasing, which indicated that the saturation adsorption capacity had been reached. The total amount of CO taken-up by the sample was calculated by quantifying the area of the peaks with the total number of CO moles present in the 250 μL loop filled with 5% CO in He. The resulting CO/Pt value was taken as a measure of the metal dispersion. It is known that, for platinum catalysts, the adsorption stoichiometry CO/Pt(s) is 1 for a wide range of dispersions.[13] Accordingly, the catalyst used in this study had a metal dispersion of 93%, in good agreement with EXAFS data previously reported.[27]

2.3. Temperature-Programmed Desorption (TPD) of Tetralin (TL), *cis*-Decalin (CD), and *trans*-Decalin (TD). TPD experiments of adsorbed TL, CD, and TD were conducted to determine the apparent heats of adsorption of the three molecules. This common method was first suggested by Cvetanomic et al.[28] while the use of the technique has been reviewed by Falconer et al.[29] The TPD runs were conducted in the same system as the dynamic CO chemisorption. The only modification was the addition of a saturation liquid trap where He is saturated with the corresponding hydrocarbon. First, 30 mg of sample was pretreated at 623 K in 100 SCCM of H_2 for 1 h. After the pretreatment, the sample was cooled in He to room temperature. This was followed by 5 mL injections of the carrier gas saturated with the hydrocarbon, sent over the catalyst every 5 min. The injections were stopped when the signal of hydrocarbon was detected, indicating the breakthrough. The weakly adsorbed hydrocarbon was removed by flowing He until the mass spectrometer signal went back to the baseline. Then, the sample was linearly heated to 573 K at a heating rate of 10K/ min. The m/e = 104 was monitored to determine the evolution of TL, while m/e = 67 was used to monitor both CD and TD. The amount of desorbed hydrocarbon was calibrated with 5 mL pulses of the hydrocarbon vapor in He, at a known vapor pressure.

2.4. Kinetic Data Collection. The kinetic experiments were conducted in a $^3/_4$ in. stainless steel reactor equipped with a thermowell to insert the thermocouple into the center of the bed. The catalytic activity was measured at three temperatures, 553, 563, and 573 K, at a pressure of 500 psig and at a H_2/aromatic molar ratio of 30. A measured amount of catalyst sample was physically mixed with inert alumina and placed in the center of the reactor between layers of 3 mm glass beads. The liquid feed was composed of 30 wt % of TL (Acros, 98+%) in dodecane as solvent (DO; Aldrich, 99%) plus 10 ppm of sulfur, with S being added in the form of dibenzothiophene (DBT; Aldrich, 99%).

The catalyst was first reduced under 225 SCCM of H_2 at 500 psig and 573 K for 2 h. After the pretreatment, when the reaction temperature was different from 573 K, the reactor was cooled in H_2 to the specified reaction temperature. Then, 10 mL/h of liquid feed was introduced to the reactor using a high-pressure D-500 Isco pump. The products were collected in a water-cooled trap and analyzed online by a HP6890 gas chromatograph with FID detector using an HP-5 column. The amount of catalyst used was varied in order to cover a wide range of space times, expressed as the W/F ratio, where W is the mass of catalyst and F is the flowrate of TL (mol/h). The reactor was operated and analyzed as an integral reactor, to cover a wide range of conversions. For each specified W/F, the kinetic data was collected at 4 h after the feed was started, using fresh catalyst each time. The conditions for intrinsic rate measurement were determined experimentally. Each experimental point is an average of 2−3 runs.

From the analysis shown in Figure 1, it was concluded that, to avoid external mass transfer resistance effects, the liquid feed rate should be greater than 10 mL/h. Likewise, it was determined that, to avoid internal mass transfer resistances, the diameter of particle should be equal or smaller than 0.4 mm (in all the kinetic studies, particles of 0.34 mm were used). Also, to ensure that the reactor was nearly isothermal across the bed, the

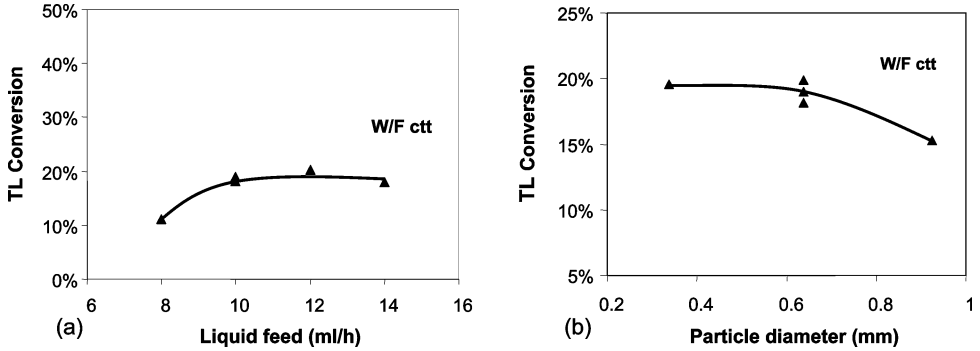

Figure 1. (a) Test for external mass transfer resistance. (b) Test for internal mass transfer resistance, at constant $W/F = 2.2$ and 573 K. Symbols are experimental values, and solid lines are included to guide the eye.

catalyst was diluted with an inert material. Dilution helps ensuring isothermicity, but it might introduce errors due to inhomogeneities in the solid mixture. Van Den Bleek et al.[30] have introduced a criterion to determine the allowable degree of dilution to keep the error due to dilution negligible in comparison to the experimental error. Using this criterion for the specific particle diameter, reactor length, and experimental error of this study, we find that up to a dilution of 3.5:1 there will be no significant additional error incorporated. Therefore, we used dilution ratios of about 2:1 although for the runs at very low W/F this ratio was higher, but not exceeding the recommended ratio 3.5:1 maximum ratio.

3. Results and Discussion

On the basis of the shape of the TPD profiles and according to criteria previously reported,[29] the desorption rate could be described neglecting any possible readsorption. Accordingly, the following expression was used in the evaluation of the desorption rate:

$$-\frac{\mathrm{d}\theta}{\mathrm{d}T} = \frac{k(\theta)}{\beta}\theta^n \exp\left(-\frac{E_\mathrm{d}(\theta)}{RT}\right) \qquad (3.1)$$

where θ = coverage, β = heating rate (K/s), E_d = energy of desorption (kJ/mol), and n = desorption order. A linear dependency of E_d with respect to θ was used.

$$E_\mathrm{d}(\theta) = E_0 + \alpha\theta \qquad (3.2)$$

The linear dependency of heat of adsorption with coverage (α) was found to be fairly small under the conditions of the experiment. This implies that heterogeneity among sites is small. This has been previously reported for certain metal-catalyzed reactions.[31,32] The pre-exponential term $k(\theta)$ was assumed to be constant.

The nonlinear parameters of the model were estimated using the Powell version of the Levenberg−Marquardt algorithm. The differential equation was solved using the EPISODE package of Scientist [Micromath] software. The evolution of experimental and simulated TL, CD, and TD coverage is shown in Figure 2 as a function of temperature in a linear ramp of 10 K/min. These curves are the integrated form of the TPD profiles and eq 3.1 respectively, normalized to saturation coverage. It is clear that TD desorbs at the lowest temperature, followed by CD, and finally TL. The heats of adsorption can be directly obtained from the fitting as the only adjustable parameters for each curve are

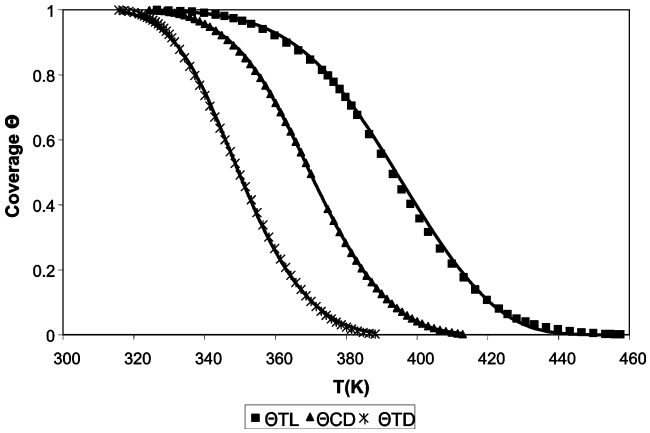

Figure 2. Experimental (points) and simulated (lines) variation of fractional coverage during desorption of tetralin (TL), *cis*-decalin (CD), and *trans*-decalin (TD), as function of temperature in a linear TPD ramp of 10 K/min.

E_d and k_d (see eq 3.1), while θ was varied from 1 to 0 and n was taken as 1.

The heat of adsorption of TL (−83.7 kJ/mol) was significantly higher than the ones resulting for CD (−66.7 kJ/mol) and TD (−65.3 kJ/mol). A higher heat of adsorption of the aromatic-containing molecule can be expected due to the rather strong interaction resulting from the parallel adsorption of aromatics on Pt surfaces.[33−35] As expected, CD and TD, without aromatic rings have lower apparent heats of adsorption and do not show significant differences between each other. These apparent heats of adsorption obtained from TPD data are within the order of magnitude expected from the rule of thumb, found from microcalorimetry studies, in which the heat of adsorption of hydrocarbons over nonmicroporous surfaces is around 4−7 kJ/mol per carbon atom.[36,37] The values of apparent heat of adsorption were used as initial estimates, for the heat of adsorption of the adsorption constants, in the kinetic fitting.

The detailed reaction path for TL hydrogenation was first described by Weitkamp.[7] A simplified reaction network takes into account three main reactions: r_1 = hydrogenation of TL to CD; r_2 = hydrogenation of TL to TD, and r_3 = isomerization of CD and TD.[6,15,16,38,39]

Under the conditions of the present study (temperature, pressure, and hydrogen/ hydrocarbon ratio), the first two reactions are essentially irreversible. However, the isomerization of CD to TD must be considered reversible. The proposed semiempirical kinetic model is described by the generalized L−H equation for

hydrogenation suggested by Kiperman.[40] For a generic hydrogenation reaction of the form

$$A + XH_2 \rightarrow B \tag{3.3}$$

the rate-limiting step is a surface reaction, so the reaction rate can be described as

$$r_i = \frac{kP_A^{n_1}P_{H_2}^{n_2}}{(L + K_A P_A + K_{H_2}P_{H_2}^{m} + K_B P_B^{n})^z} \tag{3.4}$$

In this model, which has been frequently used to describe hydrogenation of aromatics, n_1 and L are usually equal to 1; m is 0.5 for H_2 dissociative adsorption and 1 for molecular adsorption; z represents the number of surface sites required for the reaction step.[6,19−21,38]

Assuming dissociative hydrogen adsorption, as is always the case over Pt surfaces, the model results in the following expressions for the three reactions:

$$r_1 = \frac{k_1 K_{TL} K_{H_2} P_{TL}^{n_1} P_{H_2}^{n_2}}{(1 + K_{TL}P_{TL} + K_{CD}P_{CD} + K_{TD}P_{TD} + \sqrt{K_{H_2}P_{H_2}})^z} \tag{3.5}$$

$$r_2 = \frac{k_2 K_{TL} K_{H_2} P_{TL}^{n_1} P_{H_2}^{n_2}}{(1 + K_{TL}P_{TL} + K_{CD}P_{CD} + K_{TD}P_{TD} + \sqrt{K_{H_2}P_{H_2}})^z} \tag{3.6}$$

$$r_3 = \frac{k_3 K_{CD}\left(P_{CD} - \frac{P_{TD}}{K_{CD-TD}}\right)}{(1 + K_{TL}P_{TL} + K_{CD}P_{CD} + K_{TD}P_{TD} + \sqrt{K_{H_2}P_{H_2}})^z} \tag{3.7}$$

In this case, the equilibrium constant K_{CD-TD} for the reversible isomerization reaction was estimated using HSC-Chemistry-5.0 [Outokumpu Research] software. The reaction rate constants were assumed to follow Arrhenius behavior, $k = A \exp(-E/RT)$, while the apparent adsorption constants for H_2, TL, CD, and TD were expressed as

$$K_i = \exp\left(\frac{\Delta S_i^\circ}{R}\right)\exp\left(\frac{-\Delta H_i^\circ}{RT}\right) \tag{3.8}$$

The nonlinear parameter estimation of the kinetic model was performed with the same algorithm used to estimate the heat of adsorption from the TPD experiments. The ordinary differential equation system was solved with the EPISODE package of Scientist [Micromath] software as well. The objective function was the sum of the squares of the differences between experimental and calculated mole composition of TL, CD and TD at the end of the reactor.

The reactor was modeled as an isothermal plug flow reactor. As mentioned in the Experimental Section, the integral method of rate analysis was used due to the wide range of conversions investigated. The kinetic parameters were found to obey the Arrhenius law in the temperature range investigated. The kinetic fitting of all experiments was performed simultaneously for the three temperatures considered. The strong correlation between the frequency factor and the activation energy was avoided with the following reparametrization:[41]

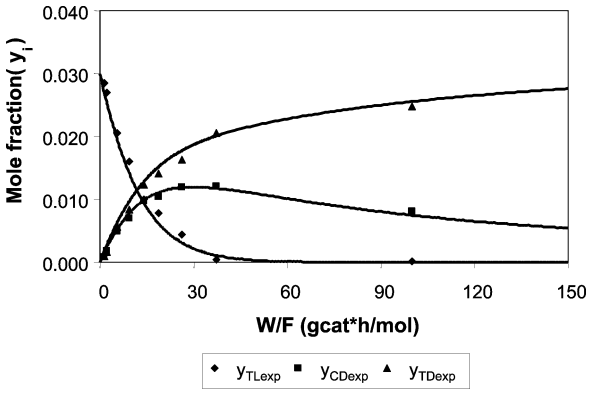

Figure 3. Product distribution for hydrogenation of tetralin at 573 K. Solid lines are the values predicted by the model. Solid points are the experimental data: diamonds represent molar fraction of tetralin (TL), squares *cis*-decalin (CD), and triangles *trans*-decalin (TD).

$$k_i = A_i \exp\left(-\frac{E_i}{R}\left(\frac{1}{T} - \frac{1}{T_{av}}\right)\right) \tag{3.9}$$

where T_{av} is the average temperature of the kinetic experiments (563 K).

The fitting parameters were limited by physical−chemical constraints. For example, frequency factors for Arrhenius equation and activation energies were forced to be positive. The initial values used in the fittings for the heats of adsorption were those obtained experimentally by TPD. Also, the entropy values were limited within the range established by the Boudart's criterion[42,43]

$$41.87 \le -\Delta S^\circ \le 51.08 - 1.4 \times 10^{-3}\Delta H^\circ \tag{3.10}$$

where ΔH° is expressed in J/mol and ΔS° in J/mol K.

The exponent in the adsorption term z was varied from 1 to 3, while the reaction order of TL was varied from 0 to 2. The reaction order with respect to hydrogen was not addressed explicitly because the concentration of H_2 under the conditions of the study was fairly constant throughout the catalyst bed. The initial estimate for the apparent heat of adsorption of H_2 was 29 kJ/mol, a typical value for hydrogen adsorption on Pt.[44] The goodness of the model, for each case, was measured by several factors such as the numerical value of the minimization function, stability of the answer (i.e., once an answer was found, the regression was re-run to see if other solutions close to the local minimum were found), agreement with physical−chemical constraints, standard error of the parameters, and study of the correlation matrix for the fit.

The best fit of the experimental data is shown in Figure 3 in the form of product distribution as a function of *W/F* at 573 K. A similarly good fitting was obtained for the other two temperatures investigated, which as mentioned above were determined simultaneously since the fitting parameters are heats of adsorption and activation energies. The value of the combined objective function for the simultaneous fitting at the three temperatures was 2.5×10^{-5}. It is clear that the selected model describes well the kinetics of the reaction in a wide range of conversion and for different temperatures, simultaneously. Also, from the best fit, the adsorption

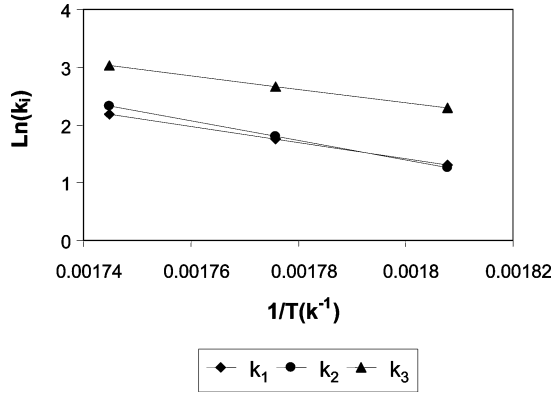

Figure 4. Arrhenius plot for the rate constants k_i (mol/gcat h).

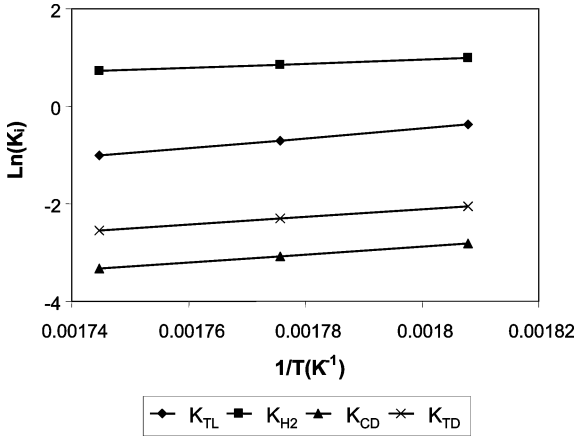

Figure 5. Temperature dependence of equilibrium adsorption constants (atm^{-1}).

Table 1. Kinetic Parameters and Standard Error for Best Model

reaction	pre-exponential term A_i (mol/gcat h)	activation energy E_i (kJ/mol)
TL → CD	5.8 ± 0.1	117 ± 6
TL → TD	6.0 ± 0.1	141 ± 5
CD ↔ TD	14 ± 1	98 ± 21

Table 2. Adsorption Parameters and Standard Error for Best Model

compd	heat of adsorption ΔH° (kJ/mol)	entropy change ΔS° (J/mol K)
TL	−84 ± 4	−155 ± 5
H_2	−34 ± 4	−53 ± 6
CD	−67 ± 4	−144 ± 6
TD	−67 ± 11	−137 ± 19

exponent z and the reaction order with respect to TL were found to be 2 and 1, respectively, in concordance with similar values previously reported in the literature.[3,40,45,46]

The kinetic parameters (pre-exponential factors and activation energies) obtained for the three reactions are summarized in Table 1, while the apparent heats of adsorption and entropy changes for all the compounds involved (TL, H_2, CD, and TD) are reported in Table 2. These parameters were used to calculate the rate and adsorption constants at different temperatures as shown in Figure 4 for the rate constants and Figure 5 for the adsorption constants.

The activation energy values obtained for the three reactions vary between 98 and 141 kJ/mol (Table 1), which are somewhat higher than the ones previously reported in the literature for this reaction.[16,46,47] This

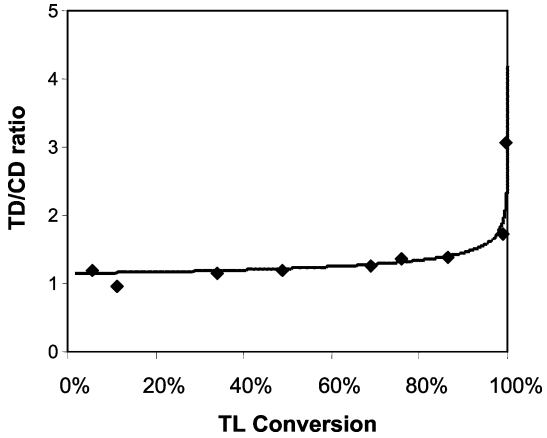

Figure 6. Model prediction (—) of the inhibition of the *cis*−*trans* reaction in comparison with experimental data (◆). Reaction temperature 573 K.

difference is reasonable if one takes into account that in the previous studies power-law or pseudo-first-order kinetic models were used; the activation energy thus obtained is in fact an apparent activation energy, which is affected by the adsorption terms and is typically lower than the true activation energy. Among the three reactions, the highest activation energy corresponds to the hydrogenation of TL to TD. This could be related to the more complicated reaction path that is required to produce TD compared to CD. As proposed by Weitkamp,[7] in order to produce TD the intermediate $\Delta_{1,9}$ Octalin (octa-hydro-naphthalene) has to either desorb and readsorb with the hydrogen facing up or roll over on the surface and be hydrogenated.[13] On the other hand since the hydrogenation of a double bond is always *syn*, CD formation does not require this last step. Interestingly, the reaction with the lowest activation energy is the isomerization of CD to TD, which, as illustrated in Figure 4, has the highest intrinsic rate constant. However, despite a lower activation energy and higher intrinsic rate constant, this reaction does not become evident until the concentration of TL in the gas phase becomes low enough to allow CD and TD to compete favorably for adsorption sites.

In a recent contribution by our group,[27] we hypothesized that site competition is one of the most important factors that govern the product distribution and relative rates in the hydrogenation of polynuclear aromatics. In the same article, we reported that for several noble-metal catalysts supported on Al_2O_3 the *cis*−*trans* ratio remained essentially constant until the TL conversion was greater than about 70−85%. After this point, the *cis*-to-*trans* isomerization clearly accelerated. This suggested that the *cis*-to-*trans* isomerization was inhibited by the presence of TL. In the present contribution, we have confirmed this premise and quantified the effect of adsorption site competition, as illustrated in Figure 6.

The large difference between the adsorption constants of TL compared to either CD or TD is mostly due to their significant differences in heat of adsorptions (Table 2). Interestingly, there are some differences among the decalin isomers. Despite having very similar heats of adsorption, the adsorption constant for TD is almost twice as high as that for CD as shown in Figure 5. The difference in entropy seems to play an important role. The entropy change resulting from the fitting was higher for CD than for TD. This disparity is physically

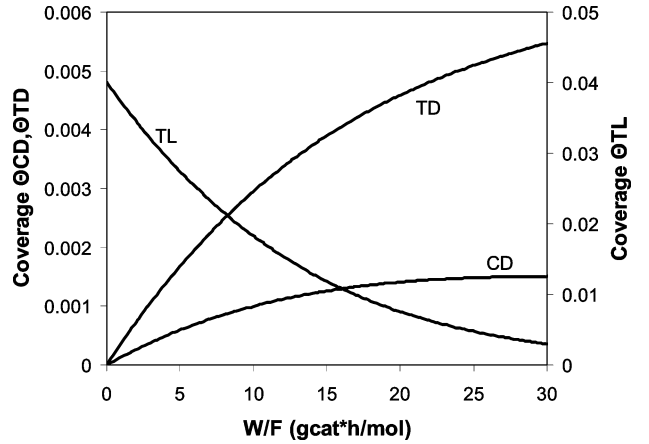

Figure 7. Predicted coverage for tetralin (TL), *cis*-decalin (CD), and *trans*-decalin (TD) as a function of *W*/*F* at 573K.

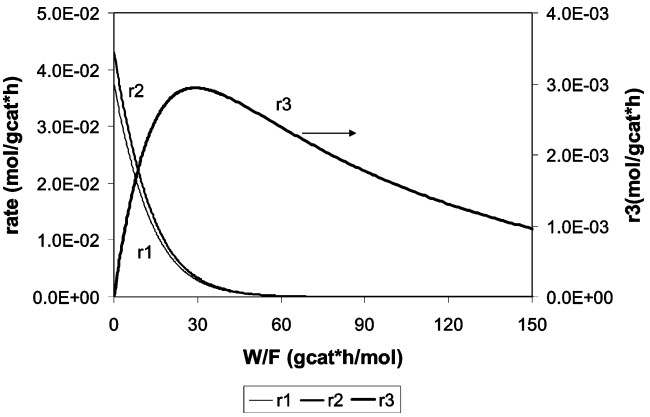

Figure 8. Reaction rate of the individual reactions (r1, r2, and r3) as a function of *W*/*F* at 573 K.

consistent with the different flexibilities exhibited by the two molecules in the gas phase. The *cis* isomer is much more flexible than the *trans* form.[7] On the adsorbed, more rigid state, the difference between the two isomers should be much less pronounced than in the gas phase. As a result, the adsorption entropy change should be larger for CD than for TD, as observed here. Finally, the heat of adsorption obtained for H_2 (-34 ± 3 kJ/mol) is not far from the initial estimate and agrees with recent microcalorimetry results reported by Cortright et al.[48] From the adsorption parameters obtained from the fitting, it is possible to predict the variation in the surface coverage of each of the components on the Pt surface as a function of *W*/*F*. While most of the surface is covered by hydrogen, which maintains coverage greater than 80% throughout the reactor, the variation in the coverage of the different hydrocarbons is significant, as illustrated in Figure 7. Near the reactor inlet, the coverage of the product decalins, particularly CD, is zero, and it remains very low across the reactor, which explains the low isomerization rate.

The net result of the site competition is clearly depicted in Figure 8 which shows the variation of the three individual rates r_1 (TL to CD), r_2 (TL to TD), and r_3 (CD to TD) as a function of space time. Although the specific rate constant of the isomerization reaction r_3 is much higher than r_1 and r_2, the isomerization can only be observed at high *W*/*F*, coincident with the decrease in TL concentration.

4. Conclusions

The kinetics analysis performed on the vapor-phase hydrogenation of TL over Pt/alumina catalyst has demonstrated the important role of adsorption site competition in determining the product distribution. Specifically, the isomerization of CD to TD is greatly inhibited until most of the TL is converted. This phenomenon can be quantitatively explained in terms of the differences in heat of adsorption obtained in this study for TL, CD, and TD. The true activation energies for the three reactions studied varies between 98 and 141 kJ/mol K. In the absence of adsorption site competition, the intrinsically fastest reaction would be the isomerization of CD to TD, but this is not shown until the hydrogenation of TL is almost complete.

Acknowledgment

We would like to acknowledge Oklahoma Center for Advancement of Science and Technology (OCAST) and ConocoPhillips for financial support. We also thank Dr. Paul Maier for proofreading the manuscript.

Literature Cited

(1) Pollack, A. In *NOx and PM Emissions, Predictions of Emission Inventory Models and Diesel's Share*, The Future of Diesel: Scientific Issues 2000 Air Pollution Symposium, Dedham, Massachusetts, 2000; MIT Energy Laboratory: Dedham, Massachusetts, 2000.

(2) Larson, B. In *The Future of Diesels: Scientific Issues*, The Future of Diesel: Scientific Issues 2000 Air Pollution Symposium, Dedham, Massachusetts, 2000; MIT Energy Laboratory: Dedham, Massachusetts, 2000.

(3) Stanislaus, A.; Cooper, B. H. Aromatic hydrogenation catalysis: A review (vol 36, pg 75, 1994). *Catal. Rev.—Sci. Eng.* **1996**, *38*, 159−159.

(4) Unzelman, G. H. In NPRA Annual Meeting; 1987.

(5) Asim, M. Y. K. D. A.; Zoller, J. R.; Platenga, F. L.; Lee, S. L. In *Hydrotreating for ultra-low aromatics in distillates*, AKZO Catalyst Seminar, 1991.

(6) Girgis, M. J.; Gates, B. C. Reactivities, Reaction Networks, and Kinetics in High-Pressure Catalytic Hydroprocessing. *Ind. Eng. Chem. Res.* **1991**, *30* (9), 2021−2058.

(7) Weitkamp, A. W. Stereochemistry and mechanism of hydrogenation of naphthalenes on transition metal catalysts and conformational analysis of the products. *Adv. Catal.* **1968**, *18*, 1−110.

(8) Cooper, B. H.; Donnis, B. B. L. Aromatic saturation of distillates: An overview. *Appl. Catal., A* **1996**, *137*, 203−223.

(9) Barbier, E. L.-P. P.; Marecot, J. P.; Boitiaux, J.; Cosyns, F.; Verna. *Adv.Catal.* **1990**, *37*, 279.

(10) Arcoya, A. C., A.; Fierro, J. L. G.; Seoane, X. L. Comparative study of the deactivation of Group VIII metal catalysts by thiophene poisoning in ethylbenzene hydrogenation. *Stud. Surf. Sci. Catal.* **1991**, *68*, 557−64.

(11) Yasuda, H.; Yoshimura, Y. Hydrogenation of tetralin over zeolite-supported Pd−Pt catalysts in the presence of dibenzothiophene. *Catal. Lett.* **1997**, *46* (1−2), 43−48.

(12) Santikunaporn, M. H. J. E.; Jongpatiwut, S.; Resasco, D. E.; Alvarez, W. E.; Sughrue, E. L. Ring opening of decalin and tetralin on HY and Pt/HY zeolite catalysts. *J. Catal.* **2004**, *228*, 100−113.

(13) Augusto, C. C. C.; Zotin, J. L.; Faro, A. D. Effect of sulfur or nitrogen poisoning on the activity and selectivity of Y-zeolite-supported Pt−Pd catalysts in the hydrogenation of tetralin. *Catal. Lett.* **2001**, *75* (1−2), 37−43.

(14) Qian, W. H.; Shirai, H.; Ifuku, M.; Ishihara, A.; Kabe, T. Reactions of tetralin with tritiated molecular hydrogen on Pt/Al_2O_3, Pd/Al_2O_3, and Pt−Pd/Al_2O_3 catalysts. *Energy Fuels* **2000**, *14* (6), 1205−1211.

(15) Sapre, A. V.; Gates, B. C. Hydrogenation of Aromatic-Hydrocarbons Catalyzed by Sulfided CoO-MoO_3-Gamma-Al_2O_3—Reactivities and Reaction Networks. *Ind. Eng. Chem. Process Des. Dev.* **1981**, *20* (1), 68−73.

(16) Huang, T. C.; Kang, B. C. Kinetic-Study of Naphthalene Hydrogenation over Pt/Al_2O_3 Catalyst. *Ind. Eng. Chem. Res.* **1995**, *34* (4), 1140−1148.

(17) Chang, J. R.; Chang, S. L. Catalytic properties of gamma-alumina-supported Pt catalysts for tetralin hydrogenation—Effects of sulfur-poisoning and hydrogen reactivation. *J. Catal.* **1998**, *176* (1), 42−51.

(18) Chiou, J. F.; Huang, Y. L.; Lin, T. B.; Chang, J. R. Aromatics Reduction over Supported Platinum Catalysts. 1. Effect of Sulfur on the Catalyst Deactivation of Tetralin Hydrogenation. *Ind. Eng. Chem. Res.* **1995**, *34* (12), 4277−4283.

(19) Rautanen, P. A.; Aittamaa, J. R.; Krause, A. O. I. Liquid-phase hydrogenation of tetralin on Ni/Al_2O_3. *Chem. Eng. Sci.* **2001**, *56* (4), 1247−1254.

(20) Rautanen, P. A. L. M. S.; Aittamaa, J. R.; Krause, A. O. I. Liquid-phase hydrogenation of naphthalene on Ni/Al_2O_3. *Stud. Surf. Sci. Catal.* **2001**, *133*, 309−316.

(21) Lylykangas, M. S.; Rautanen, P. A.; Krause, A. O. I. Liquid-phase hydrogenation kinetics of multicomponent axomatic mixtures on Ni/ Al_2O_3. *Ind. Eng. Chem. Res*. **2002**, *41* (23), 5632−5639.

(22) Rautanen, P. A.; Lylykangas, M. S.; Aittamaa, J. R.; Krause, A. O. I. Liquid-phase hydrogenation of naphthalene and tetralin on Ni/Al_2O_3: Kinetic modeling. *Ind. Eng. Chem. Res.* **2002**, *41* (24), 5966−5975.

(23) Dumesic, J.; Amiridis, M.; Goddard, S.; Rekoske, J.; Rudd, D.; Trevino, A. Microkinetics Of Metal-Catalyzed Reactions. *Abstr. Pap. Am. Chem. Soc.* **1989**, *197*, 79-Iaec.

(24) Dumesic, J.; Topsoe, N.; Slabiak, T.; Morsing, P.; Clausen, B.; Tornqvist, E.; Topsoe, H.; Sinev, M.; Vanommen, G.; Deboer, M.; Holmlid, L.; Bond, G.; Vonhippel, L.; Forzatti, P.; Armor, J.; Nam, I.; Bell, A.; Blancon, J. Microkinetic Analysis Of The Selective Catalytic Reduction (Scr) Of Nitric-Oxide Over Vanadia/Titania-Based Catalysts. *Stud. Surf. Sci. Catal.* **1993**, *75*, 1325−1337.

(25) Ovesen, C.; Clausen, B.; Hammershoi, B.; Steffensen, G.; Askgaard, T.; Chorkendorff, I.; Norskov, J.; Rasmussen, P.; Stoltze, P.; Taylor, P. Microkinetic analysis of the water-gas shift reaction under industrial conditions. *J. Catal.* **1996**, *158* (1), 170−180.

(26) Dahl, S.; Sehested, J.; Jacobsen, C.; Tornqvist, E.; Chorkendorff, I. Surface Science Based Microkinetic Analysis Of Ammonia Synthesis Over Ruthenium Catalysts. *J. Catal.* **2000**, *192* (2), 391−399.

(27) Jongpatiwat, S.; Li, Z. R.; Resasco, D. E.; Alvarez, W. E.; Sughrue, E. L.; Dodwell, G. W. Competitive hydrogenation of polyaromatic hydrocarbons on sulfur-resistant bimetallic Pt−Pd catalysts. *Appl. Catal., A* **2004**, *262* (2), 241−253.

(28) Cvetanovic, R. J.; Yoshimitsu, A. Application of a temperature-programmed desorption technique to catalyst studies. *Adv. Catal.* **1967**, *17*, 103−149.

(29) Falconer, J. L.; Schwarz, J. A. Temperature-Programmed Desorption and Reaction—Applications to Supported Catalysts. *Catal. Rev.—Sci. Eng.* **1983**, *25* (2), 141−227.

(30) Vandenbl, Cm.; Vanderwi, K.; Vandenbe, Pj. Effect Of Dilution On Degree Of Conversion In Fixed Bed Catalytic Reactors. *Chem. Eng. Sci.* **1969**, *24* (4), 681.

(31) Corma, A.; Llopis, F.; Monton, J. B.; Weller, S. W. Comparison of Models in Heterogeneous Catalysis for Ideal and Non-Ideal Surfaces. *Chem. Eng. Sci.* **1988**, *43* (4), 785−792.

(32) Ostrovskii, V. E. "Paradox of heterogeneous catalysis": Paradox or regularity? *Ind. Eng. Chem. Res.* **2004**, *43* (12), 3113−3126.

(33) Saeys, M.; Reyniers, M. F.; Marin, G. B.; Neurock, M. Density functional study of the adsorption of 1,4-cyclohexadiene on Pt(111): origin of the C−H stretch red shift. *Surf. Sci.* **2002**, *513* (2), 315−327.

(34) Morin, C.; Simon, D.; Sautet, P. Density-functional study of the adsorption and vibration spectra of benzene molecules on Pt(111). *J. Phys. Chem. B* **2003**, *107* (13), 2995−3002.

(35) Morin, C.; Simon, D.; Sautet, P. Trends in the chemisorption of aromatic molecules on a Pt(111) surface: Benzene, naphthalene, and anthracene from first principles calculations. *J. Phys. Chem. B* **2004**, *108* (32), 12084−12091.

(36) Eder, F.; Lercher, J. A. Alkane sorption in molecular sieves: The contribution of ordering, intermolecular interactions, and sorption on Bronsted acid sites. *Zeolites* **1997**, *18* (1), 75−81.

(37) van Bokhoven, J. A.; Tromp, M.; Koningsberger, D. C.; Miller, J. T.; Pieterse, J. A. Z.; Lercher, J. A.; Williams, B. A.; Kung, H. H. An explanation for the enhanced activity for light alkane conversion in mildly steam dealuminated mordenite: The dominant role of adsorption. *J. Catal.* **2001**, *202* (1), 129−140.

(38) Korre, S. C.; Klein, M. T.; Quann, R. J. Polynuclear Aromatic-Hydrocarbons Hydrogenation. 1. Experimental Reaction Pathways and Kinetics. *Ind. Eng. Chem. Res.* **1995**, *34* (1), 101−117.

(39) Schmitz, A. D.; Bowers, G.; Song, C. S. Shape-selective hydrogenation of naphthalene over zeolite-supported Pt and Pd catalysts. *Catal. Today* **1996**, *31* (1−2), 45−56.

(40) Kiperman, S. L. Some problems of chemical kinetics in heterogeneous hydrogenation catalysis. *Stud. Surf. Sci. Catal.* **1986**, *27*, 1−52.

(41) Froment, G. F. Model Discrimination and Parameter Estimation in Heterogeneous Catalysis. *AIChE J.* **1975**, *21* (6), 1041−1057.

(42) Boudart, M. 2-Step Catalytic Reactions. *AIChE J.* **1972**, *18* (3), 465.

(43) Vannice, M. A.; Hyun, S. H.; Kalpakci, B.; Liauh, W. C. Entropies of Adsorption in Heterogeneous Catalytic Reactions. *J. Catal.* **1979**, *56* (3), 358−362.

(44) Cusumano, J. A.; Dembinsk, Gw.; Sinfelt, J. H. Chemisorption and Catalytic Properties of Supported Platinum. *J. Catal.* **1966**, *5* (3), 471.

(45) Koussathana, M.; Vamvouka, D.; Economou, H.; Verykios, X. Slurry-Phase Hydrogenation of Aromatic-Compounds over Supported Noble-Metal Catalysts. *Appl. Catal.* **1991**, *77* (2), 283−301.

(46) Rousset, J. L.; Stievano, L.; Aires, F. J. C. S.; Geantet, C.; Renouprez, A. J.; Pellarin, M. Hydrogenation of tetralin in the presence of sulfur over gamma-Al_2O_3-supported Pt, Pd, and Pd−Pt model catalysts. *J. Catal.* **2001**, *202* (1), 163−168.

(47) Ho, T. C. Hydrogenation of Mononuclear Aromatics over a Sulfided $Ni-Mo/Al_2O_3$ Catalyst. *Energy Fuels* **1994**, *8* (5), 1149−1151.

(48) Cortright, R. D.; Watwe, R. M.; Spiewak, B. E.; Dumesic, J. A. Kinetics of ethane hydrogenolysis over supported platinum catalysts. *Catal. Today* **1999**, *53* (3), 395−406.

Received for review January 21, 2005
Revised manuscript received July 30, 2005
Accepted August 10, 2005

IE0500873